Journal of Catalysis 278 (2011) 1–7

Contents lists available at ScienceDirect

Journal of Catalysis

journal homepage: www.elsevier.com/locate/jcat

Synthesis of PVP-stabilized Pt/Ru colloidal nanoparticles by ethanol reduction and their catalytic properties for selective hydrogenation of *ortho*-chloronitrobenzene

Manhong Liu [a,*], Jin Zhang [a], Jinqiang Liu [b], William W. Yu [c,*]

[a] College of Materials Science and Engineering, Qingdao University of Science and Technology, Qingdao 266042, China
[b] Department of Materials Science and Engineering, Nanjing University of Science and Technology, Nanjing 210094, China
[c] State Key Laboratory on Integrated Optoelectronics, College of Electronic Science and Engineering, Jilin University, Changchun 130012, China

ARTICLE INFO

Article history:
Received 13 September 2010
Revised 9 November 2010
Accepted 10 November 2010
Available online 28 December 2010

Keywords:
Pt/Ru
Nanoparticles
Ethanol reduction
Hydrogenation
Ortho-chloronitrobenzene
Ortho-chloroaniline
Catalysis

ABSTRACT

Stable poly(N-vinyl-2-pyrrolidone)-stabilized Pt/Ru colloidal nanoparticles (PVP-Pt/Ru) were prepared via ethanol reduction of $H_2PtCl_6{\cdot}6H_2O$ and $RuCl_3{\cdot}nH_2O$. The average diameters of the nanoparticles with different molar ratio of Pt/Ru were in a range of 2.1–2.8 nm with narrow size distributions. X-ray photoelectron spectroscopy verified that both Pt and Ru were in the metallic state and Ru was rich on the surface. These nanoparticles were employed to selectively hydrogenate *ortho*-chloronitrobenzene at 298 K and 0.1 MPa hydrogen pressure. They showed high activity [TOF was in the range of $0.8–5.3 \times 10^{-2}$ $mol_{o\text{-CNB}}/(mol_{M,surface\ atom})$ s] and high selectivity (93–99%) to *ortho*-chloroaniline (*o*-CAN) for the reaction, which were composition-dependent. The selectivity to *o*-CAN monotonously increased, but the activity of the catalyst decreased with the increasing proportion of Ru in Pt/Ru colloidal catalysts. PVP-1Pt/4Ru nanoparticles exhibited the highest selectivity of 99.0% to *o*-CAN at a complete conversion.

1. Introduction

Colloidal dispersions of metallic nanoparticles are of continuous interest because of their fascinating catalytic [1], electronic [2], and optical properties [3], which differ from both the single metal atoms and the bulk metals. For catalytic applications, bimetallic colloidal nanoparticles are important considering the formation of new catalytic sites, the variation of the electronic structure, and the synergistic effects induced by a second metal component [4]. A bimetallic system of great interest is Pt/Ru, because of its usefulness as a methanol oxidation catalyst in direct methanol fuel cells (DMFC) [5,6], hydrogenation, and hydrogenolysis reactions [7].

In general, a synthesis method can strongly influence the structure, dispersity, morphology, and eventually the performance of a catalyst [8,9]. Supported high surface area catalysts are mostly prepared by (co)precipitation. Nevertheless, the preparation of alloyed particles with diameters less than 50 Å is by no means trivial, and it is desirable to find alternate methods of producing small bimetallic particles with defined particle sizes and narrow size distribution. Colloidal metal particles prepared from molecular precursors are usually small and exhibit a narrow size distribution. Several strategies to make nanosized metal colloids with different reductants, such as sodium borohydride [10], organoboride [11], alcohols [12], and polyols [13,14], have been explored.

Pt precursors can be easily reduced to zero-valent metal through low boiling point alcohol reduction, but the reduction of Ru^{3+} by low boiling point alcohols (such as ethanol) does not work. Liu et al. [15] reported the preparation of poly(N-vinyl-2-pyrrolidine) (PVP)-stabilized Pt/Ru bimetallic colloids (PVP-Pt/Ru) by $NaBH_4$ reduction. Tu and Liu [16] reported that PVP-Pt/Ru bimetallic colloids with small and narrow size distributions could be synthesized by polyol reduction with microwave irradiation at higher temperatures. However, there is little research about the preparation of PVP-Pt/Ru colloidal nanoparticles with low boiling point alcohols, such as ethanol. If there are metallic seeds, the reduction in Ru^{3+} can take place on the seed surface to produce zero-valent Ru metal nanoparticles autocatalytically. It would be deduced that zero-valent PVP-Pt/Ru bimetallic colloids could be successfully prepared by co-reducing the corresponding metal salts.

Aromatic chloroamines are important intermediates in the production of herbicides, dyes, and drugs. Their traditional syntheses through a metal–acid reduction in Bechamp's reaction produce a great amount of metal oxide waste and toxic by-products that

* Corresponding authors. Fax: +86 532 8402 2814.
E-mail addresses: liumanhong68@126.com (M. Liu), wyu6000@gmail.com (W.W. Yu).

0021-9517/$ - see front matter © 2010 Elsevier Inc. All rights reserved.
doi:10.1016/j.jcat.2010.11.009

are harmful to the environment. A suitable route is the selective hydrogenation of the corresponding chloronitro compounds over metal catalysts [17], but it is hard to avoid dehalogenation reactions [18].

As is well known, Pt can undergo a fast reduction of the nitro group but with low selectivities [18,19]. Ru is cheaper than the other noble metals and is more selective for this reaction, but its catalytic activity is generally low. So, efforts for the improvement of the catalytic activity of Ru catalysts are expected [20,21]. Liu et al. [21] investigated the selective hydrogenation of *ortho*-chloronitrobenzene (*o*-CNB) to *ortho*-chloroaniline (*o*-CAN) over a PVP-stabilized Ru colloid (PVP-Ru). Nearly 100% selectivity to *o*-CAN was obtained at 100% conversion of *o*-CNB at 320 K and 4.0 MPa. Zuo et al. [22] reported that Ru nanoparticles supported on SnO_2 colloidal particles exhibited high selectivity to *o*-CAN at 333 K and 4.0 MPa. But these works could not be accomplished at atmospheric pressure and room temperature.

It has been reported that conventional supported Pt/Ru bimetallic catalysts have quite different catalytic performances from supported Pt and Ru in selective hydrogenation of cinnamaldehye, because of the synergistic effect of Pt/Ru bimetallic particles [23]. Giroir-Fendler et al. [23] found that the catalytic properties of the Pt-Ru catalysts (in which Pt and Ru were homogeneous in particles) strongly depended on the composition of the catalyst and the coincidence increase in selectivity and activity were well accounted for by a mechanism of activation of the carbonyl bond where both Pt and Ru atoms at the surface of the particle are involved. They explained that Ru atoms, which are more electropositive than Pt atoms, act as an adsorption site for the oxygen atom of the carbonyl; thus, Pt atoms became more reactive toward hydrogen dissociated. Liu et al. [15] found that the PVP-Pt/Ru bimetallic colloids prepared by $NaBH_4$ reduction were more stable than Ru colloids, and their activities were two orders of magnitude greater than that of Ru colloids, but the selectivities were only a little bit higher than that of Pt in selective hydrogenation of *o*-CNB at 303 K and 0.1 MPa of hydrogen.

In this work, PVP-Pt/Ru nanocatalysts were prepared by co-reduction of the two metal precursors in a refluxing mixture of water and ethanol. The selective hydrogenation of *o*-CNB to *o*-CAN over a series of the as-prepared PVP-Pt/Ru colloidal catalysts reached 99.0% selectivity to *o*-CAN at 100% conversion of *o*-CNB at 298 K and atmospheric pressure; the catalytic activity was much higher than published results.

2. Materials and methods

2.1. Materials

Hydrogen hexachloroplatinate(IV) hexahydrate ($H_2PtCl_6{\cdot}6H_2O$) and ruthenium chloride hydrate ($RuCl_3{\cdot}nH_2O$, Ru content $\geqslant$37.5%, determined through a literature method [24]) of analytical grade were supplied by Beijing Chemicals Co. Poly(N-vinyl-2-pyrrolidone) (PVP, average molecular weight 10,000) was purchased from Shanghai Chemicals Co. Hydrogen (H_2) with a purity of 99.999% was generated by an extra-pure hydrogen generator HA-300. *o*-CNB was recrystallized in ethanol before use. Water was distilled and deionized before use. Other reagents were of analytical grade purity and were used as received.

2.2. Preparation of PVP-Pt/Ru colloidal nanoparticles

PVP (0.146 g, 1.31×10^{-3} mol, as monomeric unit), $RuCl_3{\cdot}nH_2O$, and $H_2PtCl_6{\cdot}6H_2O$ with a total amount of 6.55×10^{-5} mol were dissolved in a mixed solvent of water and ethanol (the ration of volume was 9:1) in a 100 mL round-bottomed flask to form a dark red homogeneous solution. The whole volume of solution was 56 mL. The solution was heated to boiling and kept refluxing in a silicon oil bath. Vigorous stirring was maintained all the time. A homogeneous dark brown solution of colloidal dispersion of PVP-Pt/Ru was obtained after 3 h. A series of colloidal nanoparticles with different compositions were synthesized by varying the molar ratio of Pt/Ru. The colloidal solutions were evaporated to dryness with a rotated evaporator under reduced pressure below 50 °C.

2.3. Instruments and characterization

Ultraviolet–Visible absorption spectra were recorded on a Varian Cary 500 UV–Vis-NIR Spectrophotometer; One milliliter of the colloidal solution was diluted to 5 mL with distilled water before measurement.

Transmission electron microscopy (TEM) photographs were taken by using a JEOL-2100 electron microscope. Specimens were prepared by placing a drop of the colloidal dispersion on a copper grid covered with a perforated carbon film and then evaporating the solvent. The particle diameters were measured from the enlarged TEM photographs. The particle size distribution histogram was obtained on the basis of the measurements of about 300–400 particles.

X-ray Photoelectron Spectroscopy (XPS) were obtained using an Axis Ultra spectrometer (Kratos, UK). A mono Al Kα (1486.6 eV) X-ray source was used at a power of 225 W (15 kV, 15 mA). To compensate for surface charge effects, binding energies were calibrated using C_{1s} hydrocarbon peak at 284.8 eV. The samples were prepared by drying the Pt/Ru colloidal dispersion via rotatory evaporation.

2.4. Catalytic hydrogenation of o-CNB

Hydrogenation of *o*-CNB was performed at 298 K and 0.1 MPa of hydrogen pressure in a 250-mL three-neck round-bottomed flask. The reaction temperature was kept constant by external circulation of a thermostat within ±0.1 °C. The reaction was performed at a stirring rate of 1400 rpm. The high stirring rate was to ensure that the reaction was performed free of any significant mass transport or diffusion limitation. Typically, 1.87×10^{-5} mol of the PVP-Pt/Ru catalyst with 0.125 g decanol (as internal standard for gas chromatography) and 13 mL methanol was activated under hydrogen with magnetic stirring at 298 K for 30 min. Air in the system was removed by sweeping the system three times with hydrogen. After activation, 2.0 mL of reactant solution (containing 1.00×10^{-3} mol *o*-CNB in methanol) was charged to the flask to start the reaction. Hydrogenation products were analyzed on a GC-1690 gas chromatography equipped with a FID detector and a DC-710 packed column.

3. Results and discussion

3.1. Preparation of PVP-Pt/Ru colloidal nanoparticles

A series of PVP-Pt/Ru colloidal nanoparticles were prepared with different ratios of the corresponding metal precursors; they were found to be stable for more than a year.

The color change of these PVP-Pt/Ru nanoparticles in the preparation process was similar to the reported results [12]. The solution of corresponding metal salts was heated quickly to boiling (normally in 5 min) and kept refluxing for 3 h. During the course of heating, we observed a succession of color changes for the reaction solution; the final solution was dark brown (Table 1). The following color changes were observed in the cases of PVP-2Pt/1Ru and PVP-1Pt/2Ru nanoparticles (Schemes 1 and 2).

Table 1
Formation of PVP-Pt/Ru colloidal nanoparticles.[a]

No.	Pt/Ru	Color changes	Color changing time[b] (min)	Average diameter, d (nm)	Standard deviation, σ (nm)	Relative standard deviation, σ/d
1	1/0	Dark red → Light yellow → Dark brown	11	3.1	0.44	0.14
2	4/1	Dark red → Light yellow → Dark brown	10	2.5	0.38	0.15
3	2/1	Dark red → Light yellow → Dark brown	12	2.8	0.37	0.13
4	1/1	Dark red → Light yellow → Brown → Gray dark → Dark brown	24	2.5	0.42	0.17
5	1/2	Dark red → Light yellow → Brown → Deep blue → Dark brown	28	2.5	0.47	0.19
6	1/4	Dark red → Light yellow → Brown → Deep blue → Dark brown	37	2.3	0.47	0.20
7[c]	1/4	Dark red → Light yellow → Brown → Deep blue → Dark brown	82	2.1	0.58	0.28

[a] Solvent: ethanol:water = 9:1 (v:v), the solvent start refluxing after heating 5 min, the molar ratio of PVP to metal precursors was 20:1.
[b] Color changing time: time counted from the beginning of the solution heated to the color of the solution changed to dark brown.
[c] The solvent start refluxing after heating 36 min, others were in 5 min.

It can be seen that when the molar ratio of Pt to Ru was not higher than 1/1 (Pt atom ⩽50%), the color of the reaction solutions changed gradually from dark red to light yellow to brown, then to deep blue, and finally dark brown (Scheme 2). This process is similar to those of PVP-Ru colloids prepared by *n*-propanol, *n*-butanol, or polyol reduction [12,14]. However, when the molar ratios of Pt to Ru were 4/1 and 2/1, the color change process tended to resemble those of PVP-Pt colloids made by low boiling point alcohols reduction (Scheme 1) [25–27]. So increasing Pt content could shorten the time of the color change process; this indicated that more Pt favorited the reduction of Ru.

The No. 7 PVP-Pt/Ru colloid (Table 1 and Scheme 3) was prepared according to the heating procedure of the literature [12]. Noble metal salts were dissolved in a mixed solvent of water and ethanol with stirring to form a dark red homogeneous solution. The solution was heated from room temperature to reflux, and the heating was kept in the whole process (230 min) with different heating rate by controlling the output power. After the mixture was heated for 10 min, the temperature reached to 333 K with a heating rate of about 3.5 °C/min, and the solution color was unchanged (dark red). The solution color changed from dark red to orange at 17 min, and the temperature gradually reached 339 K at a heating rate of about 1 °C/min. The solution began to reflux at 36 min at a heating rate of approximate 0.7 °C/min, and the solution color then changed to brown. When the mixture kept refluxing, the solution color changed from brown to deep green (54 min) and finally to dark brown (82 min). This solution was kept refluxing for another 150 min, and a homogeneous PVP-Pt/Ru colloid dispersion was achieved without precipitates (Scheme 3).

Comparing the colloids of Nos. 6 and 7 in Table 1, it can be seen that they have the same color change process, but the time of the color change process of No. 7 was longer. This illuminated that the reduction rate increased with faster heating rate on the formation of PVP-Pt/Ru colloids. It was also found that the size distribution became narrower when increasing the heating rate; this is consistent with the observation in the synthesis of noble metal colloidal particles by microwave irradiation [13]. It was reported that the

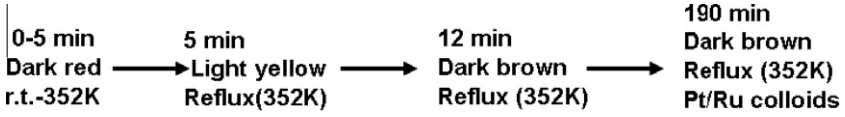

Scheme 1. Color changes of the reaction solution during the course of the PVP-2Pt/1Ru nanoparticles formation (No. 3 in Table 1).

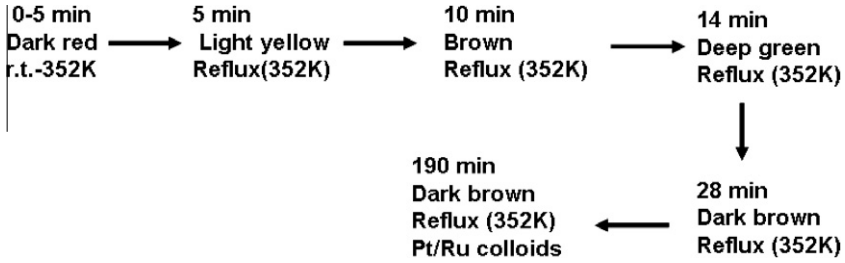

Scheme 2. Color changes of the reaction solution during the course of the PVP-1Pt/2Ru nanoparticles formation (No. 5 in Table 1).

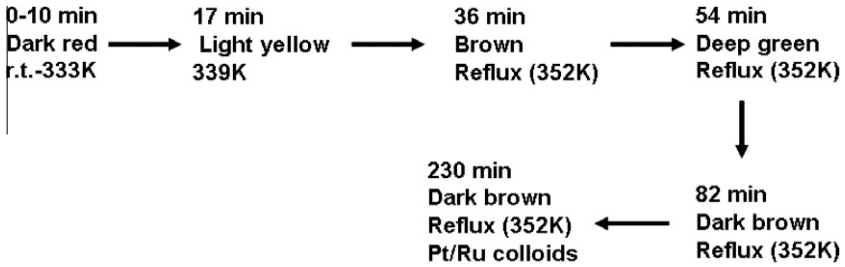

Scheme 3. Color changes of the reaction solution during the course of the PVP-1Pt/4Ru nanoparticles formation (No. 7 in Table 1).

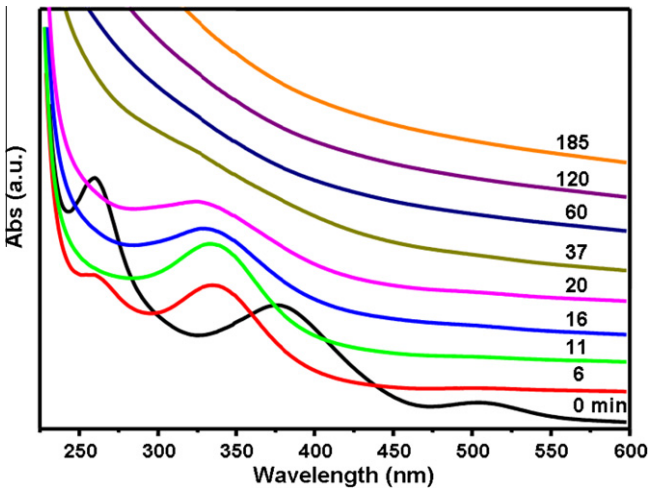

Fig. 1. UV–vis absorption spectra of the reduction of H_2PtCl_6 and $RuCl_3$ in an ethanol–water system.

microwave heating rate was about twenty times faster compared with conventional oil-bath heating, and Pt colloidal nanoparticles synthesized in methanol by microwave heating had narrower relative standard deviations (0.18) than those prepared by conventional oil-bath heating (0.25).

Colloidal dispersion of metal particles has absorption bands in the wavelength of 200–600 nm [28–30]. This is due to the excitation of plasma resonances or interband transitions, and thus a very characteristic property of the metallic nature of the particles. The formation process for PVP-Pt/Ru synthesized in the alcohol-water system was monitored by a UV–Vis spectrophotometer. Fig. 1 shows the absorption spectra of a PVP-H_2PtCl_6–$RuCl_3$ solution (Table 1 No. 6) in ethanol–water system heating with conventional method at different times. Before heating, the solution had three absorption peaks. The absorption peak at 260 nm was from the Pt(IV) species, the absorption peaks at 380 and 510 nm represented the Ru(III) species [12]. The peak at 260 nm was no longer visible when the colloid solution was heated for about 16 min, suggesting that all Pt^{4+} ions were completely reduced. The absorption peak at 510 nm disappeared immediately after heating. However, the peak at 380 nm decreased slowly and gradually shifted to short wavelength, which is similar to the literature result [12]. It implied that the Ru(III) species was gradually reduced to the corresponding zero-valent metal during this reduction process [12,14]. After about 60 min, the absorption peak at 380 nm completely disappeared, indicating that Ru^{3+} was completely reduced to Ru^0. The spectrum of the fully reduced solution displayed strong scattering absorption at wavelengths 200–600 nm, confirming the formation of PVP-Pt/Ru colloidal nanoparticles.

3.2. Characterization of PVP-Pt/Ru colloidal nanoparticles

The dependence of particle size and morphology on the molar ratio of Pt/Ru was examined by TEM. Table 1 lists the average diameters (d) and standard deviations (σ) of PVP-Pt/Ru colloids.

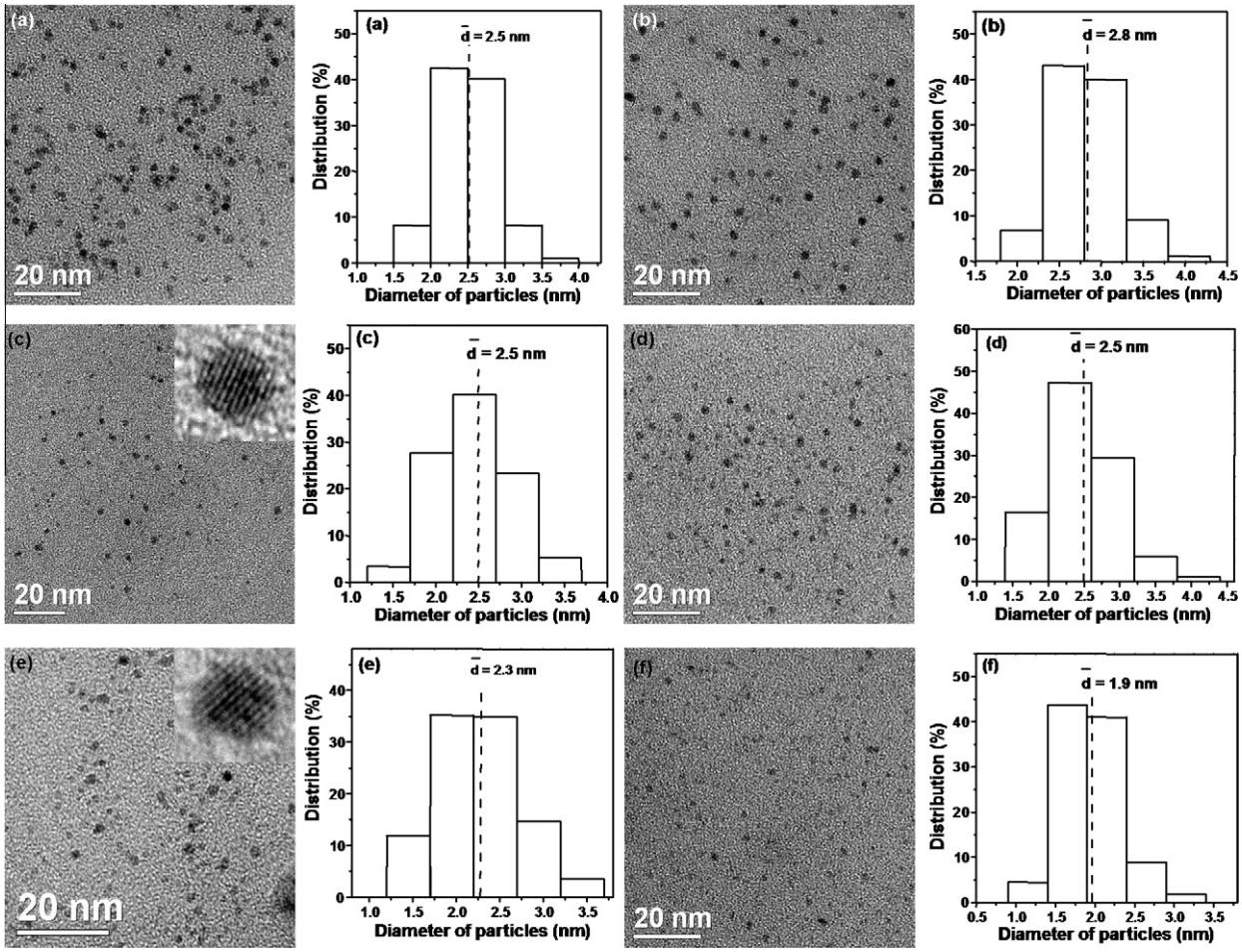

Fig. 2. TEM photographs (left) and the corresponding particle size distribution histograms (right) of PVP-Pt/Ru nanoparticles: (a) 4Pt/1Ru, (b) 2Pt/1Ru, (c) 1Pt/1Ru, (d) 1Pt/2Ru, (e) 1Pt/4Ru (No. 6 in Table 1), (f) 1Pt/4Ru (No. 7 in Table 1).

Representative TEM photographs and corresponding histograms are given in Fig. 2. According to the molar ratios of Pt to Ru in the preparation, the obtained colloidal nanoparticles were named as 4Pt/1Ru, 2Pt/1Ru, 1Pt/1Ru, 1Pt/2Ru, and 1Pt/4Ru (the numbers denote the molar ratios in the colloidal nanoparticles). The particles had small sizes about 2.1–2.8 nm in average, and no particle bigger than 4.5 nm was observed. Their standard deviations were 0.35–0.47 nm except for No. 7. The average diameter tended to decrease, and the standard deviation tended to increase with an increasing molar content of Ru in the PVP-Pt/Ru system, although the tendency was not very obvious. It can be seen from Fig. 2 that all bimetallic particles are well dispersed, and no aggregation of the bimetallic particles can be observed. These results imply that the PVP-Pt/Ru colloids have excellent stability, which is consistent with the fact that no precipitate was observed in the colloidal dispersion over one year storage at room temperature.

With the same reduction time and the same reactant, the standard deviation increases on a slower heating rate (Table 1 Nos. 6 and 7). Chen et al. [31] prepared Ru particles in ethylene glycol. They found that the reduction rate of Ru^{3+} ions (controlled by varying the reduction temperature) was important to control the particle size. Tu and Liu [13] reported that noble metal clusters synthesized by microwave heating had smaller standard deviations than those prepared by conventional oil-bath heating, because the microwave heating was much faster and more homogeneous than conventional heating. It can be seen from Table 1 that the reduction rate increases with increasing heating rate. It is therefore deduced that a faster reduction rate generally produces smaller particles with a narrower size distribution.

To confirm the formation of metallic nanoparticles, XPS was employed to determine the valence state of the obtained colloids. XPS data of 2Pt/1Ru and 1Pt/4Ru colloids (Nos. 3 and 6 in Table 1) are given in Table 2, and XPS spectra of 1Pt/4Ru colloids are also shown in Fig. 3. The binding energies of Ru $3d_{5/2}$, Ru $3p_{3/2}$, and Pt$4f_{7/2}$ in 2Pt/1Ru colloids were 279.9, 461.7, and 70.9 eV, respectively. The binding energies of Ru $3d_{5/2}$, Ru $3p_{3/2}$, and Pt $4f_{7/2}$ in 1Pt/4Ru colloids were found to be 280.0, 461.8, and 71.0 eV, respectively. They were concordant with those values for bulk Pt and Ru metals [32–35]. This demonstrated that both metal salts ($H_2PtCl_6{\cdot}6H_2O$ and $RuCl_3{\cdot}nH_2O$) were reduced to zero-valence metallic Pt and Ru, respectively.

Table 2
XPS analysis of PVP-Pt/Ru colloidal nanoparticles.

Compound	Binding energy[a] (eV)		
	Ru $3d_{5/2}$	Ru $3p_{3/2}$	Pt $4f_{7/2}$
PVP-2Pt/1Ru	279.9	461.7	70.9
PVP-1Pt/4Ru	280.0	461.8	71.0
Ru(metal)[b]	280.0		
Pt(metal)[b]			70.9

[a] The Binding energy values are referred to C_{1s}(284.8 eV).
[b] From Refs. [32–35].

For bulk materials, Pt and Ru can form alloys with Ru atomic percentage as high as 70% [36] or 79% [37]. For nanoscale materials, Pt and Ru can also form alloys [15]. Since Ru(0) cannot be obtained by ethanol reduction, it should either alloy with Pt or attach to Pt particle surface as a distinguished part. Here, HRTEM photographs are given to verify the alloy nature of the particles (inserted photographs in Fig. 2c and e). It can be seen from these images that each particle is a single crystal with all the crystal lattices through the whole particle, indicating that the alloy form of Pt and Ru in the Pt/Ru particles, rather than an attached two parts in one particle.

With respect to the surface composition of bimetallic alloy particles, Toshima et al. performed a structural analysis of PVP-Pd/Pt [30] and PVP-Pd/Au [38] colloidal nanoparticles by extended X-ray absorption fine structure (EXAFS). XPS is also an effective technique to analyze the chemical composition of particle surface [15,39]. From our XPS data, the surface composition of PVP-1Pt/4Ru was deduced to be 1:6 (atomic ratio). This indicated that Ru was concentrated on the surface in the PVP-Pt/Ru colloidal nanoparticles.

It is hypothesized that Pt precursor was reduced to zero-valent metal first by ethanol, which then helped $RuCl_3$ reduction as seeds. The composition data from XPS imply that the PVP-Pt/Ru particles have a quasi core–shell structure (core with more Pt atoms and shell with more Ru atoms). This conclusion could also be deduced through the color change and the absorption spectra during the formation of the PVP-Pt/Ru colloids in which the absorption peak at 260 nm (representing Pt^{4+} complex ion) disappeared quickly whereas the peak at 380 nm (representing Ru^{3+} complex ion) decreased slowly.

It was reported that the PVP-Pt/Ru bimetallic colloids prepared by $NaBH_4$ reduction demonstrated to be a reversed core–shell structure, with more Ru atoms in the core and more Pt atoms on the surface [15]. A very strong reductant of $NaBH_4$ made the reduction process much faster than a weak reductant of ethanol, where the solution color changed from dark red-brown to gray-blue and then to dark brown in just a few seconds, indicating that both Pt and Ru precursors could be quickly reduced to their metallic state simultaneously [15]. The surface tensions of Pt and Ru are 1865 and 2250 mN/m, respectively. According to the principle that a component with a lower surface energy tends to be concentrated on the surface, a quasi core–shell model with Ru enriched in cores, would be likely formed in the Ru/Pt colloids. But in our case, based on the color change process and the absorption spectra shown in Fig. 1, it could be deduced that $[PtCl_4]^{2-}$ disappeared quickly

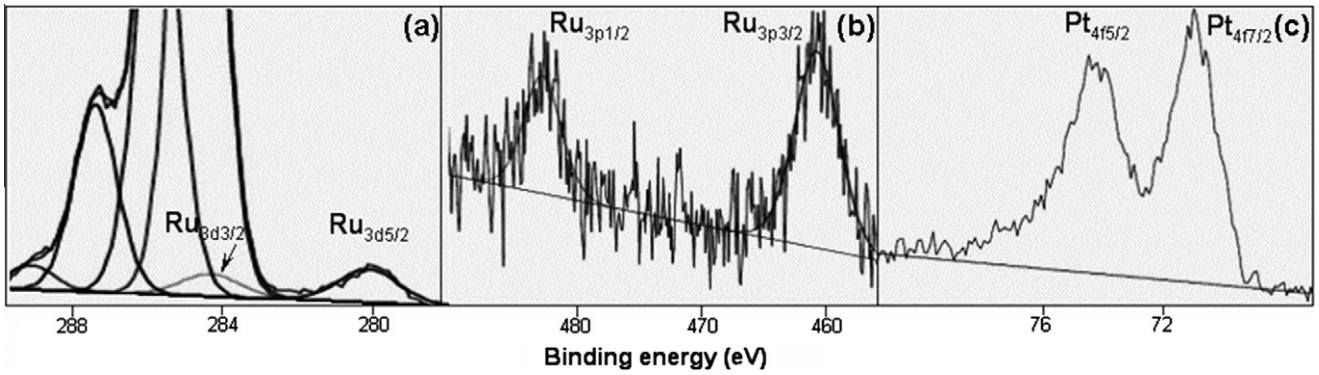

Fig. 3. XPS spectra of PVP-1Pt/4Ru: (a) Ru $3d_{5/2}$ and Ru $3d_{3/2}$, (b) Ru $3p_{3/2}$ and Ru $3p_{1/2}$, (c) Pt $4f_{7/2}$ and Pt $4f_{5/2}$.

Table 3
Selective hydrogenation of *o*-CNB over PVP-Pt/Ru colloidal catalysts.[a]

No.	Catalyst system[b]	Selectivity[c] (%)				Conversion (%) (reaction time, min)	Activity ($mol_{H2}/(mol_M)$ s)	TOF ($mol_{o\text{-}CNB}/(mol_{Pt,surface\ atom})$ s)
		o-CAN	AN	NB	Others			
1	Pt	83.1	11.0	3.9	1.9	100 (9.5)	0.28	0.26
2	4Pt/1Ru	93.1	6.8	0.1	0	99.5 (45)	0.059	4.9×10^{-2}
3	2Pt/1Ru	93.2	6.5	0.3	0	100 (53)	0.050	5.3×10^{-2}
4	1Pt/1Ru	95.4	4.4	0.2	0	100 (100)	0.027	2.2×10^{-2}
5	1Pt/2Ru	97.1	2.4	0.5	0	99.4 (160)	0.017	1.3×10^{-2}
6	1Pt/4Ru	99.0	0.2	0.8	0	100 (300)	0.009	0.8×10^{-2}

[a] Reactions were conducted at 298 K and 0.1 MPa of H_2 pressure. The overall experimental error (operation, reaction, analysis) for the component content was 5–15%, for the total conversion was less than 5%.
[b] The colloids were synthesized in a mixed solvent of ethanol:water = 9:1 (v:v).
[c] AN: aniline; NB: nitrobenzene; Others: o-chloronitrosobenzene, dichloroazoxybenzene, 2,2′-dichloroazobenzene, azobenzene.

whereas Ru^{3+} ions diminished slowly and PVP-1Pt/4Ru colloids formed after 37 min of heating. It is known that $RuCl_3$ can not be reduced to Ru(0) by ethanol solely [33]; only when H_2PtCl_6 is reduced to Pt(0) first by ethanol, the reduction in Ru^{3+} can take place on the Pt(0) seed surface to produce zero-valent Ru metal nanoparticles autocatalytically. Thus, a heterogeneously distributed particle structure of a quasi core–shell model nanoparticles with more Pt atoms in the core and more Ru atoms on the shell can be formed by ethanol reduction. The structure difference between ours and the Liu et al.'s may be due to the different reducing strengths of the reductants. The results of selective hydrogenation of *o*-CNB (see Section 3.3) are consistent with such a model.

3.3. Selective hydrogenation of o-CNB

Selective hydrogenation of *o*-CNB to *o*-CAN was carried out over the as-prepared PVP-Pt/Ru colloidal nanoparticles at 298 K and 0.1 MPa, and the results are listed in Table 3. It can be seen that the conversion of *o*-CNB was ~100% over all the PVP-Pt/Ru colloids, and the selectivity to *o*-CAN was in the range of 93.1–99.0%, which monotonously increased with the increased proportion of Ru in Pt/Ru colloidal catalysts. This selectivity is comparable to the results reported for a PVP-Ru colloidal catalyst [21,40,41] and tends to resemble PVP-Ru in catalytic performance, indicating that Ru was rich on the surface of the PVP-Pt/Ru nanoparticles. This selectivity was much higher than those of the PVP-Pt/Ru colloidal nanoparticles synthesized by $NaBH_4$ reduction [15], in which the selectivity to *o*-CAN was similar to that of PVP-Pt, in accord with their core–shell structure with more Ru atoms in the core.

The activity of our PVP-Pt/Ru colloidal nanoparticles synthesized in the ethanol–water system was in the range of 0.059–0.009 $(mol_{H2})/(mol_M)$ s by changing the molar ratio of Pt to Ru. Compared to PVP-Pt, the activity of the PVP-Pt/Ru colloidal nanoparticles was not high. However, the activity was much higher than that of PVP-Ru colloid catalyst [0.00028 $(mol_{H2})/(mol_M)$ s] [21]. PVP-4Pt/1Ru was the most active catalyst of the examined nanoparticles, with a hydrogenation rate of 0.059 $(mol_{H2})/(mol_M)$ s. In other words, the hydrogenation activity for nitro group was remarkably enhanced, while the dechlorination activity was distinctly depressed through this bimetallic combination. It was reported that the activities were 0.29 and 0.16 [$(mol_{H2})/(mol_M)$ s] for PVP-4Pt/1Ru and PVP-1Pt/4Ru synthesized by $NaBH_4$ reduction [15], which were much higher than our PVP-Pt/Ru colloidal nanoparticles. There are two possible reasons for the difference. First, the surface component was different. There was more Pt on nanoparticle surface synthesized by $NaBH_4$ reduction. This increases the activity. Second, there were boron species (the borates) presented in the nanoparticles synthesized by $NaBH_4$ reduction. This might exhibit a remarkable promotion effect on the reaction rate [41].

The activity and selectivity of bimetallic nanocatalysts are greatly influenced by their components and compositions [4]. As shown in Table 3, the selectivity to *o*-CAN monotonously increased, but the activity of the catalyst decreased with the increasing proportion of Ru in Pt/Ru colloidal catalysts. It was known from the XPS measurements of 1Pt/4Ru colloids that Ru atoms were enriched on the surface of the Pt/Ru bimetallic particles. More Ru atoms on the surface lead to a higher selectivity. The high selectivity and activity of PVP-Pt/Ru colloidal nanoparticles may also attribute to the electron transfer between these two metals. Giroir-Fendler et al. [23] proposed that Ru atoms, which are more electropositive than Pt atoms, acted as an adsorption site for the oxygen atom of the carbonyl, gave the coincidence increase in selectivity and activity of the hydrogenation of cinnamaldehyde over homogeneous Pt-Ru bimetallic particles. Similar situation may occur in our case for the HRTEM images tell us the alloy form of Pt and Ru in the Pt/Ru particles. Therefore, Ru as the electron-deficient species on the surface of the bimetallic catalysts may act as electrophilic or Lewis acid sites for the polarization and activation of the N=O bond via the interaction with the lone electron pair of the oxygen atom, favoring its hydrogenation [18]. As for the selectivity to haloaniline, its enhancement was attributed to the relative adsorption strength of halonitrobenzene on Ru increased, whereas the relative adsorption strength of haloaniline was reduced, which resulting high selectivity to *o*-CAN.

Some supported catalysts (such as Ag/SiO_2 [42], Au/SiO_2 [43], Au/ZrO_2 [44], and Ru/SnO_2 [22]) are highly selective in the hydrogenation of haloaromatic nitro compounds. However, their activities at higher reaction temperatures and higher hydrogen pressures are obviously lower than that of our PVP-Pt/Ru nanocatalysts. A few reactions over Pt/γ-Fe_2O_3 [45–47] can be operated under ambient conditions to hydrogenate chlorinated nitroarenes; their activities are not high, whereas Ir/hydrous zirconia [48] exhibits comparable selectivity with higher activity under ambient conditions. But Pt or Ir are more expensive than Ru.

Cárdenas-Lizana et al. [49–52] reported that a continuous gas-phase hydrogenation of *p*-chloronitrobenzene over Au/Al_2O_3 and Au/TiO_2 could achieve a selectivity of 100% to *p*-chloroaniline operating at 453 K. A continuous operation is generally good for high throughput. However, these reported processes have to be operated at higher temperatures, which may bring in issues such as the extra energy input, the protection and maintenance of equipment, and the safety. Considering these factors, batch reactions under room temperature may be a good alternate. Furthermore, though the work reported here is a batch operation, it is possible to convert it to a continuous reaction once we solve the catalyst separation from the products.

4. Conclusions

We reported for the first time the preparation of a series of PVP-Pt/Ru nanoparticles in ethanol–water system. TEM results showed

that the particle size could be controlled around 2–3 nm. XPS and UV–Visible spectroscopy measurements proved the complete reduction in Pt(IV) to Pt(0) and Ru(III) to Ru(0). XPS data also revealed a quasi core–shell structure with Ru enriched in the shell for these bimetallic nanoparticles. The catalytic performance of these colloidal nanoparticles depended on their compositions; the high selectivity to *o*-CAN was contributed by Ru component.

Acknowledgment

We are grateful for financial support from the National Natural Science Foundation of China (NSFC, 21077062) and the Outstanding Youth Promotive Foundation of Shandong (Contract No. 2008BS09009).

References

[1] H. Hirai, H. Chawanya, N. Toshima, React. Polym. 3 (1985) 127.
[2] V.L. Colvin, M.C. Schlamp, A.P. Alivisatos, Nature 370 (1994) 354.
[3] G. Schön, U. Simon, Colloid Polym. Sci. 273 (1995) 202.
[4] N. Toshima, Y. Wang, Langmuir 10 (1994) 4574.
[5] E.V. Spinacé, A.O. Neto, M. Linardi, J. Power Sour. 129 (2004) 121.
[6] L. Dubau, F. Hahn, C. Coutanceau, J.M. Léger, C. Lamy, J. Electroanal. Chem. 554/555 (2003) 407.
[7] J.M. Thomas, R. Raja, B.F.G. Johnson, T.J. óConnell, G. Sankar, T. Khimyak, Chem. Commun. (2003) 1126.
[8] K.Y. Chan, J. Ding, J. Ren, S. Chen, K.Y. Tsang, J. Mater. Chem. 14 (2004) 505.
[9] E. Antolini, Mater. Chem. Phys. 78 (2003) 563.
[10] M. Liu, B. He, H. Liu, X. Yan, J. Colloid Interface Sci. 263 (2003) 461.
[11] H. Bönnemann, W. Brijoux, R. Fretzen, T. Joussen, R. Koppler, B. Korall, P. Neiteler, J. Richter, J. Mol. Catal. 86 (1994) 129.
[12] Y. Zhang, J. Yu, H. Niu, H. Liu, J. Colloid Interface Sci. 313 (2007) 503.
[13] W. Tu, H. Liu, J. Mater. Chem. 10 (2000) 2207.
[14] X. Yan, H. Liu, K.Y. Liew, J. Mater. Chem. 11 (2001) 3387.
[15] M. Liu, W. Yu, H. Liu, J. Zheng, J. Colloid Interface Sci. 214 (1999) 231.
[16] W. Tu, H. Liu, Chin. J. Polym. Sci. 23 (2005) 487.
[17] V. Kratky, M. Kralik, M. Mecarova, M. Stolcova, L. Zalibera, M. Hronec, Appl. Catal. A 235 (2002) 225.
[18] B. Coq, A. Tijani, F. Figuéras, J. Mol. Catal. 71 (1992) 317.
[19] X. Yang, H. Liu, Appl. Catal. A 164 (1997) 197.
[20] A. Tijani, B. Coq, F. Figuéras, Appl. Catal. 76 (1991) 255.
[21] M. Liu, W. Yu, H. Liu, J. Mol. Catal. A 138 (1999) 295.
[22] B. Zuo, Y. Wang, Q. Wang, J. Zhang, N. Wu, L. Peng, L. Gui, X. Wang, R. Wang, D. Yu, J. Catal. 222 (2004) 493.
[23] A. Giroir-Fendler, D. Richard, P. Gallezot, Faraday Discuss. 92 (1991) 69.
[24] D.J. Miller, S.C. Srivastava, M.L. Good, Anal. Chem. 37 (1965) 739.
[25] M. Liu, M. Han, W.W. Yu, Environ. Sci. Technol. 43 (2009) 2519.
[26] W. Yu, M. Liu, H. Liu, J. Zheng, J. Colloid Interface Sci. 210 (1999) 218.
[27] H. Harai, Y. Nakao, N. Toshima, J. Macromol. Sci. Chem. A 13 (1979) 727.
[28] A.I. Kirkland, P.P. Edwards, D.A. Jefferson, D.G. Duff, Annu. Rep. Prog. Chem. 87 (1990) 247.
[29] J.A. Creighton, D.G. Eadon, J. Chem. Soc. Faraday Trans. 99 (1991) 3881.
[30] N. Toshima, M. Harada, T. Yonezawa, K. Kushihashi, K. Asakura, J. Phys. Chem. 95 (1991) 7448.
[31] Y. Chen, K.Y. Liew, J. Li, Mater. Lett. 62 (2008) 1018.
[32] C.D. Wagner, W.M. Riggs, L.E. Davis, J.F. Moulder, in: B.E. Muilenberg (Ed.), Handbook of X-Ray Photoelectron Spectroscopy, Perkin–Elmer, Physical Electronics Division, Eden Prairie, 1979, p. 106.
[33] W. Yu, M. Liu, H. Liu, X. Ma, Z. Liu, J. Colloid Interface Sci. 208 (1998) 439.
[34] W. Yu, M. Liu, H. Liu, Y. Zhang, J. Chin. Electr. Microsc. Soc. 17 (1998) 629.
[35] V.M. Desphande, W.R. Parterson, C.S. Narasimhan, J. Catal. 121 (1990) 165.
[36] V.A. Nemilov, A.A. Rudnizky, Izv. Akad. Nauk S.S.S.R. (Khim.) (1937) 33.
[37] N.V. Ageev, V.G. Kuznetsov, Izv. Akad. Nauk S.S.S.R. (Khim.) (1937) 753.
[38] N. Toshima, M. Harada, Y. Yamazaki, K. Asakura, J. Phys. Chem. 96 (1992) 9927.
[39] H. Liu, G. Mao, S. Meng, J. Mol. Catal. 74 (1992) 275.
[40] X. Yan, M. Liu, H. Liu, K.Y. Liew, N. Zhao, J. Mol. Catal. A 170 (2001) 203.
[41] X. Yan, M. Liu, H. Liu, K.Y. Liew, J. Mol. Catal. A 169 (2001) 225.
[42] Y.Y. Chen, C. Wang, H.Y. Liu, J.S. Qiu, X.H. Bao, Chem. Commun. (2005) 5298.
[43] Y.Y. Chen, J.S. Qiu, X.K. Wang, J.H. Xiu, J. Catal. 242 (2006) 227.
[44] D.P. He, H. Shi, Y. Wu, B.Q. Xu, Green Chem. 9 (2007) 849.
[45] J. Zhang, Y. Wang, H. Ji, Y. Wei, N. Wu, B. Zuo, Q. Wang, J. Catal. 229 (2005) 114.
[46] X. Wang, M. Liang, J. Zhang, Y. Wang, Curr. Org. Chem. 11 (2007) 299.
[47] M. Liang, X. Wang, H. Liu, H. Liu, Y. Wang, J. Catal. 255 (2008) 335.
[48] G. Fan, L. Zhang, H. Fu, M. Yuan, R. Li, H. Chen, X. Li, Catal. Commun. 11 (2010) 451.
[49] F. Cárdenas-Lizana, S. Gomez-Quero, M.A. Keane, Catal. Commun. 9 (2008) 475.
[50] F. Cárdenas-Lizana, S. Gómez-Quero, M.A. Keanea, Chem. Sus. Chem. 1 (2008) 215.
[51] F. Cárdenas-Lizana, Z.M. de Pedrob, S. Gómez-Quero, M.A. Keanea, J. Mol. Catal. A 326 (2010) 48.
[52] F. Cárdenas-Lizana, S. Gómez-Quero, A. Hugon, L. Delannoy, C. Louis, M.A. Keanea, J. Catal. 262 (2009) 235.